Interaction of Two Plane, Parallel Jets

G. F. Marsters*
Queen's University, Kingston, Ontario, Canada

This work reports the analysis and experimental observations of the flowfield of two plane, parallel jets that merge as they issue into stagnant surroundings. The experimental results are compared with predictions based upon a simple momentum integral analysis of the flowfield. Although the crude analysis predicts the merging of the jets reasonably well, it does not predict accurately the secondary flow entrained in the unobstructed space between the jet nozzles. The experimental data are presented in the form of similarity plots of the mean velocity and dimensionless plots of the static pressure distribution.

Nomenclature

A = area ratio, secondary to primary
J_p = momentum flux at nozzle exit plane
J_x = momentum flux for downstream stations
ℓ = nozzle length (span)
$\dot{m}$ = mass flow rate
p = static pressure
Re = Reynolds number based on jet nozzle width t_p
R = initial radius of curvature of jet trajectory
S = nozzle spacing
$\bar{S}$ = ratio of nozzle spacing to nozzle width t_p
t_p = jet nozzle width
U_p^* = nozzle exit plane velocity, expansion to freestream static pressure
U = mean flow velocity in x direction
u = x component of velocity
V_∞ = nozzle exit plane velocity, expansion to local static pressure
x = streamwise coordinate along centerline of system
x_0 = downstream distance to where centerline static pressure returns to ambient pressure
x_p = fictitious merge point
y = coordinate normal to centerline of system
$y_{1/2}$ = y value at which $U = \frac{1}{2} U_{\max}$
z = coordinate normal to ceiling and floor planes
α = coefficient related to merge point
β = angle between jet axis and system centerline
ζ_i, ζ_r = ratios of jet spreading parameters
ϕ = gross thrust augmentation
λ = velocity ratio, primary to secondary
η = dimensionless similarity variable $\sigma y/x$
ρ = density of fluid
θ = angle defined in Fig. 1
$\sigma, \sigma_i, \sigma_c$ = jet spreading parameters

Subscripts and Superscripts

∞ = freestream conditions
$1,2$ = upstream and downstream stations
e = entrained flow
m = merge point
p = primary flow quantity
t = stagnation conditions
$*$ = maximum static pressure at wall
0 = nozzle exit plane conditions
$'$ = fluctuating velocity

Received Jan. 18, 1977; presented as Paper 77-176 at the AIAA 15th Aerospace Sciences Meeting, Los Angeles, Calif., Jan. 24-26, 1977; revision received July 13, 1977.

Index categories: Nozzle and Channel Flow; Jets, Wakes, and Viscid-Inviscid Flow Interactions.

*Professor, Department of Mechanical Engineering. Member AIAA.

Introduction

WHEN two jets with parallel axes issue from nearby nozzles into still surroundings, their trajectories deviate from straight lines because of mutual entrainment of the surrounding fluid. The mechanism is the same as that which causes jets to attach to nearby walls. Plane jets issuing from large aspect-ratio slot nozzles will entrain each other, tending to merge into a single jet at some downstream station. The case of plane, parallel jets issuing from a solid wall has been examined experimentally.[1,2] That case is similar to the reattachment of a jet following a step in a wall.[3,4] Such "unventilated" reattaching jets result in recirculating flow in a low-pressure region between the nozzle exit plane and the reattachment point. The case of "ventilated" jets, e.g., jets issuing from free standing nozzles such that secondary flow can be entrained between them, has not been studied. Nonetheless, such configurations may be useful in thrust augmentors for STOL and VTOL applications.

In this work, we first present a simplified analysis of ventilated jet pairs based on mean flow quantities and integral methods. The associated experimental program will be described, and the experimental data will be compared with the predictions based on the simplified analysis.

The present analysis deals with jets that issue from self-contained nozzles such that the surrounding fluid can be entrained between the jets as well as from the region "outside" the jets. The jet axes may be inclined at an angle β with respect to the centerline of the merged jet. This symmetrical arrangement is related to the jet flap diffuser.[5] The experimental program is concentrated on the case of $\beta = 0$. Otherwise the experiments are designed to approximate closely the conditions of the analytic model.

The analysis is based on mean flow quantities and does not deal with the details of the turbulent mixing process. The "ejector" action of the system is included, however, and estimates of thrust augmentation are made.

Analysis

The analysis is restricted to plane, incompressible flows. It is assumed that the secondary flow velocity, denoted U_s, is uniform across the plane between the nozzles, and that the velocity profiles of the primary nozzles are flat. The jets are assumed to merge at some finite downstream location x_m beyond which the static pressure is uniform, and, as far as entrainment and momentum flux is concerned, the combined flow behaves like a single two-dimensional jet. The divergence angle β is constrained to be small. If the divergence angle is large enough, the jets will not merge at all. The transverse momentum of each jet is neglected.

The continuity and x-component momentum equations are written for the flow between stations 1 and 2 indicated in Fig. 1. Assuming that the mass entrainment on the outer surface of

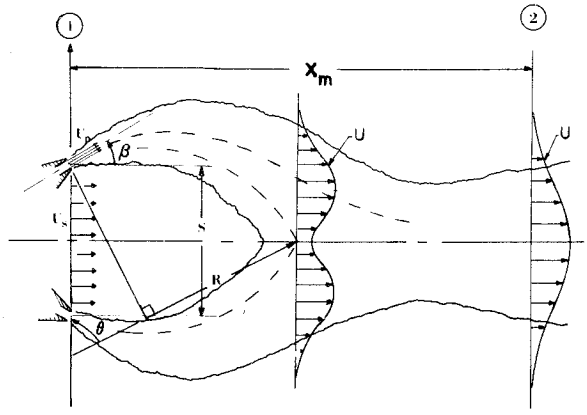

Fig. 1 Flowfield geometry.

the jets is $\dot{m}_e(x)$, we have

$$\rho\int_{-\infty}^{\infty} u\,dy = 2\rho U_p t_p + \rho U_s(S - t_p\cos\beta) + \dot{m}_e(x) \tag{1}$$

$$p_1(S + t_p\cos\beta) - p_2(S + t_p\cos\beta) = \rho\int_{-\infty}^{\infty} u^2\,dy - 2\rho U_p{}^2 t_p\cos\beta - \rho U_s{}^2(S - t_p\cos\beta) \tag{2}$$

Note that the mass flux across station 1, outside the jet boundaries, is neglected; consistent with this, the static pressure at station 1, outside the nozzle boundaries, is assumed to be ambient (p_∞). At station 1, the static pressure between the nozzles and over the nozzle exits is

$$p_1 = p_\infty - \tfrac{1}{2}\rho U_s{}^2 + \Delta p \tag{3}$$

where Δp represents the losses or the influence of any device upstream of station 1 in the secondary flow. Station 2 is taken to be sufficiently far downstream to insure that the static pressure is uniform everywhere and equal to p_∞. We define the area ratio $A = (S - t_p\cos\beta)/t_p$ and the velocity ratio $\lambda = U_p/U_s$. If $\Delta p = 0$, then combining Eqs. (2) and (3) yields, with some rearrangement,

$$2\cos\beta + \frac{(A - 2\cos\beta)}{2\lambda^2} = \frac{1}{U_p{}^2 t_p}\int_{-\infty}^{\infty} u^2\,dy$$

The integral is to be evaluated at some sufficiently large value of x where the merged jets behave like a single freejet, and so we may express the velocity distribution by[4]

$$u = \sqrt{3J_x\sigma/4\rho x}\ \operatorname{sech}^2(\sigma y/x) \tag{4}$$

with the assumption that the hypothetical origin of the jet is at the nozzle exit plane. Here, J_x is the momentum flux of the merged, self-preserving jet, evaluated at $x > x_m$; J_x is constant. The jet spreading rate is indicated by the spreading parameter σ. Noting that $U_p^2 t_p = J_p/\rho$, where J_p is the momentum flux of one of the primary jets, the integral becomes

$$\frac{3}{4}\frac{J_x}{J_p}\int_{-\infty}^{\infty} \operatorname{sech}^4\eta\,d\eta$$

where $\eta = \sigma y/x$. One then obtains the momentum equation in the following form:

$$2\cos\beta + (A - 2\cos\beta)/2\lambda^2 = J_x/J_p \tag{5}$$

Proceeding with the continuity equation, we examine the total flow into the jet over the external (outside and inside) jet surfaces. Up to the point x_m on the outer surfaces, entrainment takes place at a rate determined by the curvature[6]; beyond this point, the entrainment parameter is assumed to be σ. Thus, for the outer surfaces,

$$\dot{m}_e(x) = \int_0^{x_m}\left(\frac{d\dot{m}_e}{dx}\right)dx + \int_{x_m}^{x}\left(\frac{d\dot{m}_e}{dx}\right)dx$$

For stations downstream of x_m,

$$\frac{d\dot{m}_e}{dx} = \frac{d}{dx}\left[\rho\int_{-\infty}^{\infty}\sqrt{\frac{3J_x x}{4\rho\sigma}}\operatorname{sech}^2\left(\frac{\sigma y}{x}\right)d\left(\frac{\sigma y}{x}\right)\right]$$

Thus,

$$\int_{x_m}^{x}\left(\frac{d\dot{m}_e}{dx}\right)dx = 2\sqrt{\frac{3}{4}\frac{\rho J_x}{\sigma}}\left[\sqrt{x} - \sqrt{x_m}\right]$$

For stations upstream of x_m, a value of $\sigma_c = 13.2$ is assumed.[6] Then the entrainment rate is given by

$$\frac{d\dot{m}_e}{dx} = \frac{d}{dx}\left[\rho\sqrt{\frac{3J_p x}{4\rho\sigma_c}}\int_{-\infty}^{\infty}\operatorname{sech}^2\frac{\sigma_c y}{x}\,d\left(\frac{y\sigma_c}{x}\right)\right]$$

Therefore,

$$\int_0^{x_m}\left(\frac{d\dot{m}_e}{dx}\right)dx = \sqrt{\frac{3J_p\rho x_m}{\sigma_c}}$$

Equation (1) then becomes

$$\rho\int_{-\infty}^{\infty}\sqrt{\frac{3J_x\sigma}{4\rho x}}\operatorname{sech}^2\left(\frac{\sigma y}{x}\right)dy = 2\rho U_p t_p + \rho U_s(S - t_p\cos\beta) + \sqrt{\frac{3J_x\rho}{\sigma}}\left[\sqrt{x} - \sqrt{x_m}\right] + \sqrt{\frac{3J_p x_m\rho}{\sigma_c}}$$

On evaluating the integral and dividing by J_p, the result is

$$\sqrt{\frac{3}{4}\left(\frac{x_m}{t_p}\right)}\left[\sqrt{\frac{J_x}{J_p\sigma}} - \sqrt{\frac{1}{\sigma_c}}\right] = 1 + \frac{A}{2\lambda} \tag{6}$$

On the inner surfaces of the jets, it is clear that the secondary flow all must be entrained in a distance of, at most, αx_m, where $0 < \alpha \le 1$. On these surfaces, the spreading parameter is denoted σ_i; the value of σ_i is taken to be[6] 18.5. Assuming a uniform entrainment rate on the inner surface of both primary jets,

$$\int_0^{\alpha x_m}\frac{d}{dx}(\dot{m}_e)\,dx = \int_0^{\alpha x_m}\frac{d}{dx}\left[\int_{-\infty}^{\infty}\sqrt{\frac{3}{4}\frac{J_p x\rho}{\sigma_i}}\times\operatorname{sech}^2\frac{\sigma_i y}{x}\,d\left(\frac{y\sigma_i}{x}\right)\right]dx = \sqrt{\frac{3J_p\rho x_m\alpha}{\sigma_i}}$$

This must be just equal to the secondary flow $\rho U_s t_p A$, whence we find

$$A/\lambda = \sqrt{3x_m\alpha/\sigma_i t_p} \tag{7}$$

Eliminating x_m from (6) and combining with (5) yields

$$\frac{A}{2\lambda} = \left[\sqrt{\left[2\cos\beta + \frac{A - 2\cos\beta}{2\lambda^2}\right]\frac{\zeta_i}{\alpha}} - \sqrt{\zeta_r} - 1\right]^{-1} \tag{8}$$

where $\zeta_i = \sigma_i/\sigma$ and $\zeta_r = \sigma_i/\sigma_c$. Equation (8) may be solved for λ, provided that the value of α is fixed. Unfortunately, the distances x_m and αx_m are not determined easily, and little guidance is available for establishing α. To assist in estimating α, we make use of the pressure difference across the jets and denote as x_p the location of circular arcs drawn tangent to the centerlines of each jet at the nozzle exit plane. The initial radius of curvature R is estimated on the basis of the jet momentum and the pressure difference across the jets. With reference to Fig. 1, we can write

$$\frac{dp}{dr} = \frac{\rho U_p^2}{R} \tag{9}$$

$$S = 2R(1-\cos\theta) \tag{10}$$

$$x_p = R\sin\theta \tag{11}$$

Approximating dp/dr by $\Delta p/t_p$ and recalling that $\Delta p = \frac{1}{2}\rho U_s^2$, one obtains

$$\frac{x_p}{t_p} = 2\lambda^2 \sin\cos^{-1}\left[1 - \frac{A+\cos\beta}{4\lambda^2}\right] \tag{12}$$

It seems clear that x_p is a lower limit for the distance for merging of the jets, and that the merge point lies somewhere between x_p and x_m. The analysis proceeds as follows: Eq. (8) is solved for λ (seeking the solution by interactive computation with the aid of a programmable desktop calculator) assuming $\alpha = 1$. The value of λ obtained is used to calculate x_p [Eq. (12)]. The original value of α and the value of x_p/x_m are suitably averaged, and new values of λ and x_m are calculated. When the change in x_m lies within a predetermined tolerance (1% typically), the computation is terminated; otherwise a new value of x_p is calculated, leading to a new value for α (averaged as before), and the solution procedure is repeated. The results of these calculations are shown in Figs. 2 and 3 and will be discussed later.

Ultimately, one is interested in the thrust augmentation available with a pair of plane jets. The gross thrust augmentation ϕ is the ratio of momentum flux at the exit plane of the device to the momentum flux of the primary streams, assuming that the primary streams expand to ambient pressure p_∞ and the primary mass flux remains the same. With the primary flow stagnation pressure denoted p_t,

$$\phi = J_x/2\dot{m}_p V_\infty \tag{13}$$

where $\dot{m}_p = \rho U_p^* t_p$, and $U_p^* = \sqrt{2(p_t - p_\infty)/\rho}$. Because $V_\infty = \sqrt{2(p_t - p_l)/\rho}$, we find

$$\frac{J_p}{J_p^*} = \frac{V_\infty^2}{U_p^{*2}} = \frac{2(p_t - p_\infty) + \rho U_s^2}{2(p_t - p_\infty)} = 1 + \frac{U_s^2}{V_\infty^2}\frac{V_\infty^2}{U_p^{*2}}$$

With this result, (13) and (5) yield

$$\phi = \tfrac{1}{2}\frac{\lambda}{\sqrt{\lambda^2 - 1}}\left[2\cos\beta + \frac{A - 2\cos\beta}{2\lambda^2}\right] \tag{14}$$

Values of ϕ obtained from Eq. (14) are plotted in Fig. 2.

Experimental Program

A simple experiment was designed to test the theory outlined in the preceding paragraphs. There appear to be no experimental data in the literature for the case of interest here, although several studies of the interactions of unventilated plane jets have been reported.[1,2] These cases are similar to the reattachment of a two-dimensional jet to an offset flat wall, which has been studied by Bourque and Newman[4] and by Kumada et al.[3] Because of the "ventilation" feature allowing

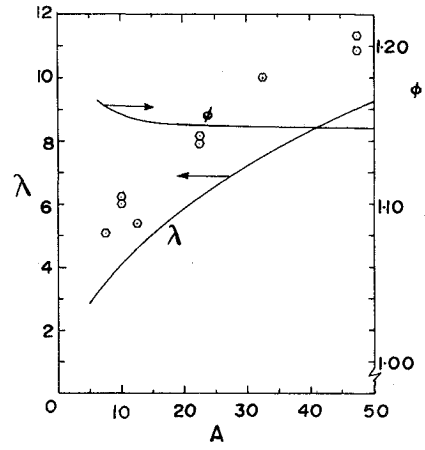

Fig. 2 Primary to secondary velocity ratio λ and thrust augmentation φ as functions of area ratio; data points for λ only.

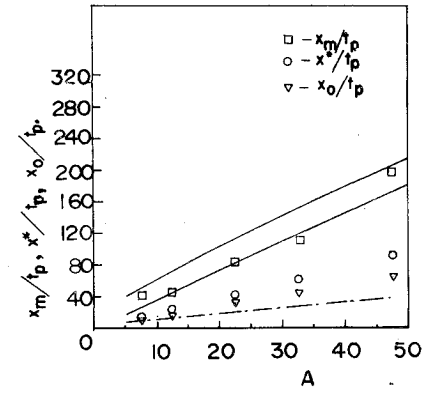

Fig. 3 Merge point location; predictions and experimental results.

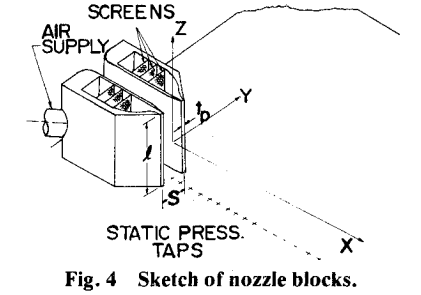

Fig. 4 Sketch of nozzle blocks.

entrainment between the jets, the present case is not comparable with Refs. 1 and 2. The mean flow characteristics of ventilated jet pairs have been observed, and the results are compared with the preceding analysis.

Jet Nozzles

The jets issued from slot nozzles of thickness $t_p = 2.54$-mm and length $\ell = 114.3$ mm. The slots are located in two identical settling chambers, constructed as shown in Fig. 4. Screens inserted in the settling chambers result in a uniform velocity along the length of the slot. Although the contraction (contraction ratio 17.25) is asymmetric, the velocity profiles are flat both across and along the jet. The 45:1 aspect ratio was considered to be adequate for two-dimensionality of flow for each jet. Trentacoste and Sforza[7] report that, even for three-dimensional jets, for aspect ratios of 40, the centerline velocity decay and the velocity profiles are typical of those for plane jets, up to about 200 jet widths downstream. For $x/t_p < 150$, the centerline velocity decay data for the nozzles shown in Fig. 4 are well fitted by the straight line

$(U_p/U)^2 = 0.165$ $(x/t_p - 3.55)$. This is in good agreement with values in the literature.[8] For downstream distances x/t_p greater than about 150, the velocity decay becomes more three-dimensional in character.

The chamber wall adjacent to the symmetry plane for the jet pair was made as thin as practicable and was chamfered at the exit, as shown in Fig. 4. Although this amounts to a slight diffuser effect for the entrained flow, a thinner wall would deform under the pressure applied to the settling chamber, resulting in a nozzle of varying width.

The jet nozzle blocks are held between two large plane surfaces ("floor" and "ceiling"). The nozzles serve as spacers at the upstream end of the flow, while spacer blocks are used downstream. The lower plane contains a row of some 30 static pressure taps along the centerline of the nozzle pair which permit observation of the static pressure in the region between the jets and along the centerline of the merged jet. A traversing apparatus allows transverse traverses (hot wire or pitot tube) to be carried out at any location up to 300 nozzle widths (t_p) downstream of the nozzle exit plane.

Velocity Profiles from Slot Nozzles

Lateral and spanwise total head traverses were carried out to determine the degree of uniformity of the flow from these nozzles. One nozzle block was subjected to several detailed traverses. The other simply was checked to ascertain that the flow was uniform.

Spanwise traversing revealed a very flat profile, with a slight (about 0.75% of mean velocity) bulge near one end. Over the middle 90% of the span, the average velocity was 98.9% of the maximum value observed, and the standard deviation was 0.0036. Lateral traverses were carried out near midspan and at stations approximately ¼ span from the edges of the jet nozzle. These traverses revealed remarkably flat profiles. Some rounding of the profiles was observed near the edges of the jet; this is attributed to the probe size. The probe o.d. was almost 0.40 t_p. Over the middle 80% of the nozzle thickness, however, the velocity was generally within 1% of the maximum value. All traverses were carried out at velocities of the order of 36 m/sec, corresponding to a Reynolds number based on jet thickness t_p of about 6000.

Test of Reattachment to Plane Wall

It is worth noting that it is extremely important that the jet nozzles span the interval between the floor and ceiling planes. The first set of nozzle blocks did not; they incorporated sidewalls such that the aspect ratio was only 40:1. A gap of about 6.4 mm existed between the edge of the jet and the floor or ceiling at the nozzle exit. This permitted air to "leak" into the low-pressure region between the jets. This discrepancy was found only after some experimentation, and it was decided to check the behavior of a jet attaching to a wall following a step, as in Refs. 3 and 4. Only when the nozzle blocks were redesigned to span between the floor and ceiling could the results indicated by Fig. 4 of Ref. 3 be reproduced. Kumada et al.[3] deduced an empirical relation to predict the reattachment point. For the conditions used in this experiment, with the jet-to-wall offset $h/t_p = 15$, the observed reattachment point was within 3% of the predicted location.

Test of Two-Dimensionality of Flow

Because of boundary layers forming at both top and bottom walls and because of the low pressure existing between the two plane jets upstream of the merge point, the two-dimensionality of the flow had to be checked. Indeed, at points where the jet width is comparable to the distance between the floor and ceiling planes, one may expect that the two-dimensional character of the flow will be compromised seriously. To examine this, traverses at points near the bottom and top planes were carried out. The results are reported elsewhere.[9] The principle conclusion from the investigation of the profiles at three planes is that there is no evidence of gross departure from two-dimensionality in the jet velocity profiles either upstream or downstream of the merge point.

Observations in Merging Jet Flows

The data observed in these experiments fall into three categories: 1) wall static pressure distributions; 2) mean velocity traverses; and 3) turbulence intensities. Additional tests were carried out to examine the effects of unequal flows and of varying the Reynolds number.

Wall Static Pressure

For each spacing used, wall static pressures were recorded. Although most velocity traverses were carried out at $R_e = 12{,}000$, wall static pressures were observed for higher and lower Reynolds numbers. The Reynolds number effect is observed to be negligible over the range $8600 < Re < 15{,}000$.

Several plots of wall static pressure vs downstream location are shown in Fig. 5. These resemble, not surprisingly, the wall static pressure profiles reported in Refs. 1-3. However, for unventilated flows, the static pressure is not minimum at the nozzle exit plane, whereas in the present case the pressure rises steadily from the nozzle exit plane, reaching a maximum at a downstream distance that depends upon the nozzle spacing. The locations of these static pressure maxima are shown (x^*/t_p) in Fig. 3, along with predictions of the merge point of the jets.

An examination of the wall static pressure data suggest that the downstream distance at which the maximum pressure is observed is proportional to the spacing between the jets. Thus, when the x values corresponding to maximum static pressure are normalized with respect to the area ratio A, the maximum pressures tend to converge to a single value of x/A.

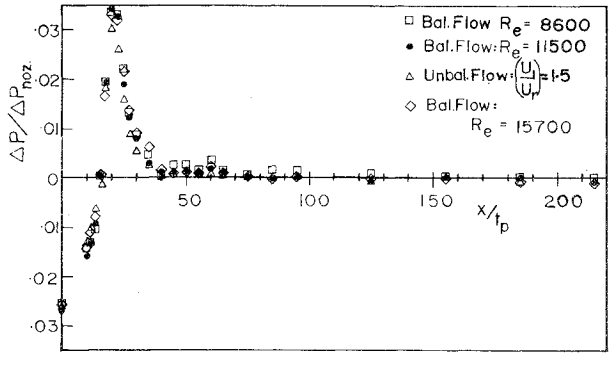

Fig. 5 Wall static pressure distributions along centerline for several flows ($S = 11$).

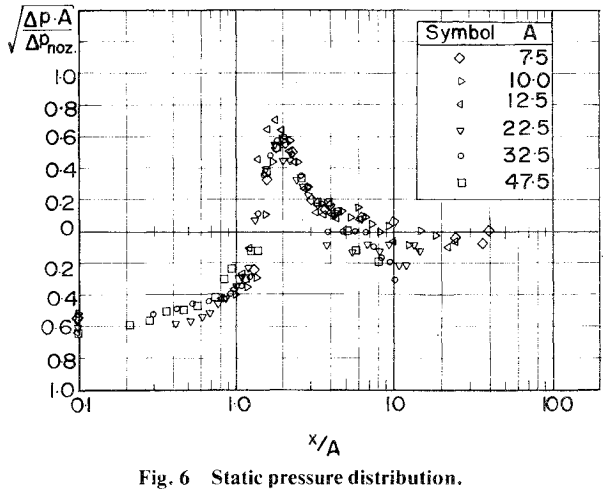

Fig. 6 Static pressure distribution.

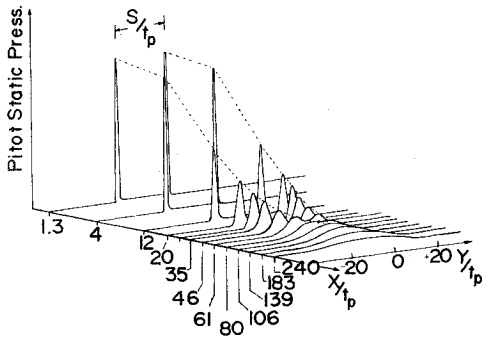

Fig. 7 Dynamic pressure distribution in flowfield.

The preceding results suggest that the pressure behavior should be plotted with x/A as the independent variable, and the pressure distribution plotted in the nondimensional form $\sqrt{(\Delta P/\Delta P_{noz})A}$. Representative static pressure data for each spacing are plotted in Fig. 6. The data collapse rather well onto a single curve, except at large values of x/A, where considerable scatter is evident. Although it cannot be claimed that the data follow a single universal curve, this presentation is expected to be helpful in locating reattachment points for other ventilated plane jet flows.

Figure 7 is a tracing of a "three-dimensional" plot of the velocity pressure distribution. This figure is of value in visualizing the merging of the jets. The twin peaks first start to decay independently with downstream distance, and they also approach each other. For the case shown, the two peaks have converged at $x/t_p \simeq 80$, while the wall static pressure maximum occurs at about $x/t_p = 40$, and the static pressure is within 1% of ambient at $x/t_p = 80$.

Mean Velocity Traverses

Velocity traverses using pitot tubes, pitot static tubes, and hot wires were carried out for six spacings and at numerous downstream stations. The selection of downstream stations was determined from the observed static pressures, so that the region of jet merging could be examined closely.

The near region (within the potential core) traverses reveal "top-hat" profiles. An example profile obtained at $x/t_p = 2.7$ is shown in Fig. 8, along with data for the x component of the fluctuating velocity. The mean velocity is based upon hot-wire measurements. The hot wires were calibrated in situ with the aid of pitot tube data recorded on the same traverses. The full lines connect mean flow data points; the dashed lines connect turbulence data points.

The mean flow data indicate that the flow is well "balanced." In the region between the jets, the secondary flow is clearly evident; in this case $\lambda \simeq 8$. There is also evidence of a wake in the secondary flow from the interior walls of the jet nozzle blocks. As expected, the turbulence intensity $(\overline{u'^2}/U^2)^{1/2}$ is very low in the core region of each jet and in the secondary flow.

Each jet exhibits the behavior that one would expect from a single jet. The only unusual features are the (predicted) secondary flow and the wakes shed from the interior nozzle block walls.

Because jet velocity profiles exhibited a high degree of similarity except near the merge point, many of the data are presented in the form of similarity plots, e.g., U/U_{max} vs $y/y_{1/2}$, where $y_{1/2}$ is the value of y at which $U = \frac{1}{2}U_{max}$. The mean flow profiles for points upstream of the merge point are displayed in Fig. 9, while the downstream profiles are shown in Fig. 10. Typical examples of velocity profiles in the nonsimilar regions of the flow, e.g., near the nozzle exit and in the merging region, are given in Fig. 11. In this latter figure, the y coordinate is normalized with respect to the spacing S.

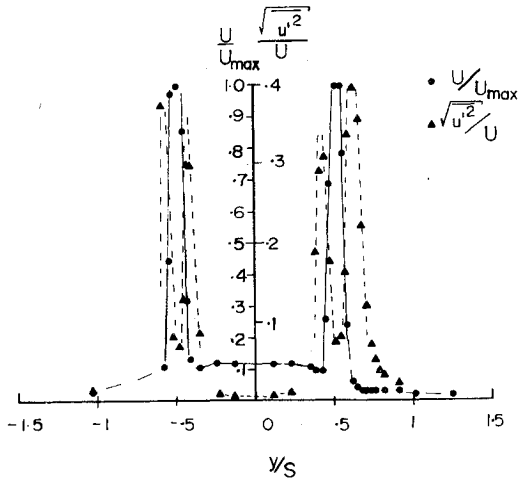

Fig. 8 Mean velocity and turbulence intensity at $x/t_p = 2.7$.

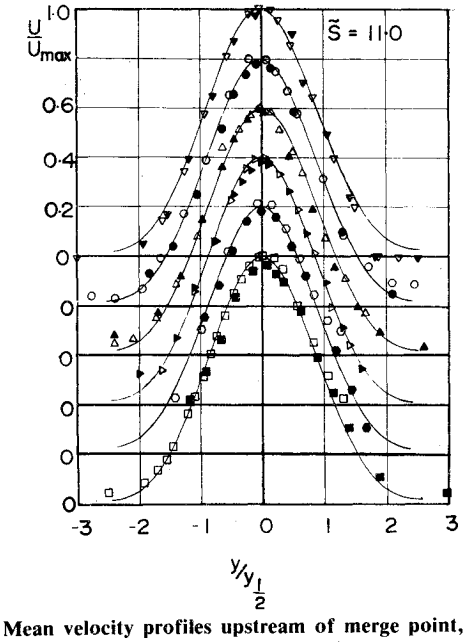

Fig. 9 Mean velocity profiles upstream of merge point, pitot tube data: $x/t_p = 15$, ▽, ▼; $= 20$, △ ▲, $= 25$ ⬡, ⬢; hot-wire data $x/t_p = 12.7$, ○ ●; $= 17.7$, ▷, ▶; $= 22.7$, □ ■; open symbols refer to right jet.

The velocity traverse data yield the behavior of the centerline velocity with downstream distance and the trajectories of the jet centerlines. In plane turbulent jets, the centerline velocity decay is inversely proportional to $(x/t_p)^{1/2}$. Figure 12 shows the centerline velocity decay for the jet pairs at various spacings. This plot indicates that, downstream of the potential core region, the jets first of all decay as if they were truly two-dimensional flows. Subsequently, at an x/t_p value that depends on S, the decay rate decreases through the merging region, followed by a return to the decay rate characteristic of two-dimensional jets. This latter region lends further support to the contention that, at least within the range of x values of this study, the jet flow retains a high degree of two-dimensionality. This plot suggests that, except for the merging region, one should expect to find the structure of the jet flow (e.g., the turbulence field) comparable to that of a single free jet. In the merging region, significant effects may be expected due to the large pressure gradients (both axial and lateral) associated with the turning of the jet flows. However, the structure should be very nearly the same as that observed in Refs. 1 and 2.

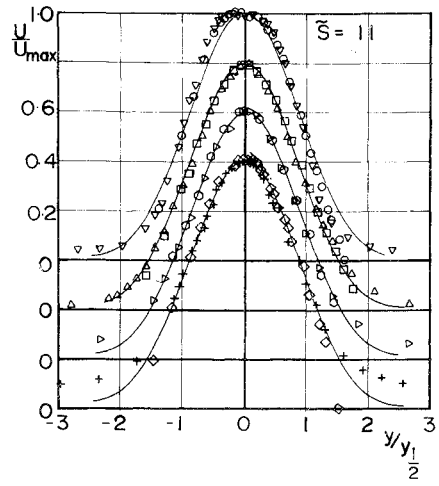

Fig. 10 Mean velocity profiles downstream of merge point: pitot tube/hot-wire data: $x/t_p = 50$, ○ / ▽ = 90, □ / △ ; = 140, ⬭ / ▷ ; = 200, ◇ / +.

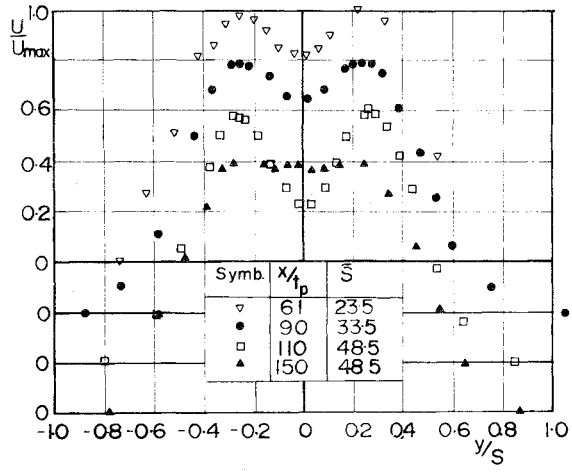

Fig. 11 Velocity distributions in the merge region.

The mean velocity data also allow the determination of the rate of spread of the jets. This is characterized in the usual fashion by plotting the jet half-width ($y_{½}/t_p$) vs downstream distance x/t_p. For the near field, the jet spreading rate is linear, as is the case for free single jets. The spreading rate is approximated by the expression $y_{½} = 0.1\ (x - x_0)$, where $x_0 = -4t_p$. This is in good agreement with other published results for planar jets.[8]

Asymmetric flows and Reynolds Number Effects

Occasional asymmetries were observed in the jet flows, wherein the difference in the peak velocities upstream of the merge point was a few percent. (If the unbalance exceeded about 5%, the flows were regulated and the run started over; establishing a balanced flow at constant delivery pressure is a time-consuming task.) To determine the gross effects of such an unbalanced flow, the centerline static pressures were observed while the velocity ratio between left and right jets was varied from about 1.5 to about 0.7. The results for a single spacing, $\tilde{S} = 11$, are shown in Fig. 5. The centerline static pressures are insensitive to asymmetric flows over the range investigated.

Although the majority of experiments were carried out at nozzle exit plane velocities of about 67 m/sec, a few observations were made at higher and lower velocities, all within the range of incompressible flow, which yielded a range of Reynolds numbers of 8600 to 15,700. These investigations consisted of observing the centerline static pressures for a

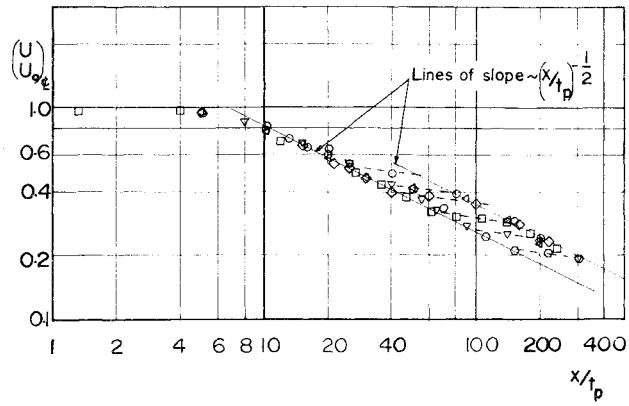

Fig. 12 Centerline velocity decay of merging plane jets: ○ $-\tilde{S} = 8.5$; ◁ $-\tilde{S} = 11$; ◇ $-\tilde{S} = 13.5$, □ $-\tilde{S} = 23.5$; ▽ $-\tilde{S} = 33.5$; ⬭ $-\tilde{S} = 48.5$

single spacing, $\tilde{S} = 11$. The resulting data are plotted in Fig. 5. From this figure it is evident that the centerline static pressure distribution is virtually unaffected by variations of Reynolds number in the range $8600 < Re < 15{,}700$.

Discussion

The simplified integral analysis provides surprisingly good predictions of the behavior of the mixing jets. The entrainment rates are overpredicted (Fig. 2), but reasonable predictions of the merging process (Fig. 3) are obtained despite the crudeness of the calculation. There is little incentive to attempt to refine the calculation, since the simplest procedure at this point would be to develop a numerical computational scheme (or apply one of the commercially available programs) to this problem. The most forbidding task then would be to develop a satisfactory turbulence model for this particular flow.

The observations of the flowfield indicate that the mean flow quantities (velocity profiles) quickly become self-preserving, and the two jets behave quite independently of each other upstream of the merge region, despite the fairly high curvature of each jet centerline. A rather complex pressure field exists in the merge region wherein the centerline static pressure rises steeply to a maximum, then falls off rather less precipitiously, eventually returning to atmospheric pressure. The rising pressure field, upstream of the merge point, constitutes a rapid diffusion process for the secondary flow. There was no indication in this work of separation, despite this rapid diffusion. Indeed, the flowfield was observed to exhibit a high degree of two-dimensionality, even when important lateral characteristic lengths were about equal to the span of each jet. Measurements were made far enough downstream to encompass most regions of interest.

Summary and Conclusions

The mean flow quantities for the incompressible mixing of two plane, parallel, ventilated jets have been examined experimentally and compared with predictions based on a crude integral model of the flow. The agreement is surprisingly good.

Except for the merging region, the velocity profiles exhibit self-preserving behavior, both upstream and downstream of the merging region. The flowfield maintains a high degree of dimensionality even far downstream.

The centerline velocity decay and jet spreading rates are essentially the same as for the planar jets issuing into still surroundings for the pair of jets upstream of the merge point. The static pressure distribution along the centerline of the flowfield is quite insensitive to unbalanced (asymmetric) flows and is unaffected by variations in Reynolds numbers over the range $8600 < Re < 15{,}700$.

Acknowledgments

This work was supported by the National Research Council of Canada under Grant No. A4310. Interest in this problem was stimulated by Doug Garland, De Havilland Aircraft of Canada Limited, while the author was Senior Industrial Fellow at De Havilland.

References

[1] Miller, D. R. and Comings, E. W., "Force-Momentum Fields in a Dual-Jet Flow," *Journal of Fluid Mechanics*, Vol. 7, Feb. 1960, pp. 237-256.

[2] Tanaka, E., "The Interference of Two-Dimensional Parallel Jets," (2nd Rept.), *Bulletin of the Japan Society of Mechanical Engineers*, Vol. 17, July 1974, pp. 920-927.

[3] Kumada, M., Mabuchi, I., and Oyakawa, K., "Studies on Heat Transfer to Turbulent Jets with Adjacent Boundaries," (3rd Rept.), *Bulletin of the Japan Society of Mechanical Engineers*, Nov. 1973, pp. 1712-1722.

[4] Bourque, C. and Newman, B. G., "Reattachment of a Two-Dimensional Incompressible Jet to an Adjacent Flat Plate," *Aeronautical Quaterly*, Vol. XI, Aug. 1960, pp. 201-232.

[5] Morel, J. P. and Lissaman, P.B.S., "Jet Flap Diffuser: A New Thrust Amplifying Device," *Journal of Aircraft*, Vol. 8, July 1971, pp. 491-495.

[6] Sawyer, R. A., "Two-Dimensional Reattaching Jet Flows including the Effects of Curvature on Entrainment," *Journal of Fluid Mechanics*, Vol. 17, Dec. 1963, pp. 481-498.

[7] Trentacoste, N. and Sforza, P., "Further Experimental Results for Three-Dimensional Free Jets," *AIAA Journal*, Vol. 5, May 1967, pp. 885-891.

[8] Gutmark, E. and Wygnanski, I., "The Planar Turbulent Jet," *Journal of Fluid Mechanics*, Vol. 73, Feb. 1976, pp. 465-495.

[9] Marsters, G. F., "A Study of the Interaction of Plane Parallel Jets," Dept. of Mechanical Engineering, Queen's Univ., Kingston, Ontario, Thermosciences Rept. 1/77, June 1977.